Measuring the Glass Transition Temperature of Vapor Phase Infiltrated AlO_x-PS-*r*-PHEMA Organic-Inorganic Hybrid Thin Film Materials

James T. Bamford[†], Ronald A. Smith[‡], Collen Z. Leng[†], Will R. Gutekunst[*‡], Mark D. Losego[*†]

[†]School of Materials Science and Engineering, [‡]School of Chemistry and Biochemistry, Georgia Institute of Technology, Atlanta, Georgia 30332, United States

For Table of Contents Use Only:

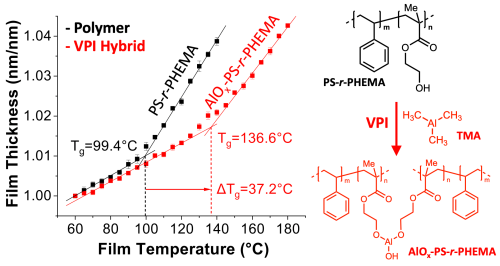

ABSTRACT: Glass transition temperature (T_g) is a fundamental property of a polymer that defines its upper service temperature for structural applications and is often indicative of its other thermophysical features. This paper investigates how vapor phase infiltration (VPI), which infuses polymers with inorganic species to create organic-inorganic hybrid materials, affects the material's glass transition temperature. We examine VPI of aluminum oxide (Al_2O_3 or AlO_x) into poly(styrene-*r*-2-hydroxyethyl methacrylate) (PS-*r*-PHEMA) random copolymer thin films using trimethylaluminum (TMA) and water (H_2O) precursors. Our VPI precursors are intended to be unreactive towards the styrene monomer units and highly reactive towards the HEMA monomer units. Experiments were conducted on PS-*r*-PHEMA thin films (200 nm)

spun-cast onto silicon wafers and infiltrated at 100 °C with 4 hr exposure times. Copolymers with varying fractions of HEMA units were investigated, from 0 mole % to 20.2 mole % HEMA. Volumetric swelling of the films after VPI and aluminum oxide film thicknesses after pyrolysis both confirm higher metal oxide loading in polymers with higher HEMA fractions. T_g was measured by tracking film thickness as a function of temperature using spectroscopic ellipsometry. The glass transition temperature is found to increase significantly with metal oxide loading. Copolymers with 0.0%, 3.0%, 7.7%, 11.5%, and 20.2% HEMA units experienced 6, 8, 22, 37, and 46 °C increases in T_g respectively. Changes in T_g at low HEMA compositions fit the Fox-Loshaek model for crosslinking phenomena, which, along with a dissolution study on these materials, suggests that VPI is crosslinking the PS-*r*-PHEMA polymer. This study demonstrates that VPI is useful for altering the thermophysical and thermochemical properties of polymer materials, likely in many different form factors including thin films, coatings, membranes, foams, fibers, and fabrics.

INTRODUCTION

Vapor phase infiltration (VPI) is a gas-phase materials modification process that infuses polymers with inorganic constituents to form new organic-inorganic hybrid materials, with the inorganic constituents often homogeneously mixed at the sub-nanometer level. During VPI, a polymer substrate is exposed to vapor-phase inorganic (e.g., metalorganic) precursors that diffuse into a polymer's free volume and become physically or chemically entrapped within the polymer. The physicochemical structure of the resulting hybrid material depends upon the polymer chemistry, metalorganic precursor chemistry, and VPI process conditions (e.g., temperature, partial pressure, and sequence timing). These variables can influence the amount of inorganic infiltrated as well as the nature of polymer-inorganic interactions. Metalorganic precursors may directly react with the polymer to form primary chemical bonds to the organic, or they may simply lose volatility due to decomposition and/or reaction with delivery of a secondary co-reactant, leading to physical entrapment in the polymer network. These chemical modifications have the potential to form inorganic chemical crosslinks between polymer chains and/or form inorganic side groups or unbound clusters that impede polymer reptation. Potential applications of VPI-created hybrid materials include oil sorbents[1], photovoltaics[2], lithography masks[3], antireflective coatings[4], and chemical separation membranes[5].

The thermophysical properties of VPI-created hybrid materials have not been extensively explored. For example, to the best of our knowledge, no changes in glass transition temperature (T_g) have previously been reported. T_g is a fundamental property of a polymer that defines its upper service temperature in many applications and is reflective of its physicochemical

features. T_g marks the transition from a glassy state of low chain mobility to a rubbery state of high chain mobility in solid amorphous polymers. Crosslinking (the chemical binding of multiple polymer molecules to each other) is known to drastically reduce polymer chain mobility, thereby increasing T_g[6-9]. Because T_g has a significant impact on mechanical properties, crosslinking can theoretically increase the maximum service temperature of structural polymer glasses, such as polycarbonate windows[10] or PVC pipes[11]. Considering these two phenomena (T_g and crosslinks), we expect that if VPI were to add inorganic crosslinks to the polymer, the resulting hybrid material would likely have a higher T_g than the parent polymer.

This investigation establishes a relationship between vapor phase infiltration and polymer glass transition temperature. We use poly(styrene-*r*-hydroxyethyl methacrylate) random copolymers (PS-*r*-PHEMA) with varying compositions to control metal oxide loading. In this material system, TMA most likely reacts with the hydroxyl groups in HEMA. Polymers with higher concentrations of HEMA monomer units should bind more inorganic alumina to their chains during VPI. We then measure the T_g of these different hybrid compositions by tracking their thermal expansion as a function of temperature and compare to the neat polymer to understand the relationship between the physicochemical structure of the hybrid material and its T_g.

EXPERIMENTAL METHODS

PS-*r*-PHEMA Synthesis and Characterization

All polymerization reactions were carried out using dry solvents under a nitrogen atmosphere. Dry and degassed N,N-dimethylformamide (DMF) was obtained from JC Meyer solvent purification system. 2,2′-Azobisisobutyronitrile (AIBN, Matric Scientific, 97% purity) was recrystallized from ethanol. All monomers: Styrene (Sty, Acros Organics, 99%, Stabilized) and 2-hydroxyethyl methacrylate (HEMA, Tokyo Chemical Industry, >95%, Stabilized with MEHQ) were passed through a column of basic alumina prior to polymerization. Solvents for precipitation were used as received: Methanol (MeOH, Fisher Scientific, >99.8%) and Hexane (Hex, Fisher Scientific, >98.5%). Unless stated otherwise, all other reagents were purchased at the highest commercial quality and used without further purification.

All polymers were synthesized using thermally-induced free radical polymerization. For styrene homopolymer (0% HEMA), 1 ml of 42 mg/mL stock AIBN solution in dry DMF (42 mg, 0.24 mmol, 1 eq), 6.5 mL of dry DMF, and 13.8 mL of styrene (12.5 g, 120 mmol, 500 eq) was added to a 40 mL vial. The vial top was perforated with a long purge needle and a short venting needle. The solution was then purged with nitrogen gas for 15 min. After the purge, the vial top was sealed

with viscous superglue, covered in electrical tape, and wrapped with parafilm ensuring an airtight seal. The vial was then placed into an oil bath at 60 °C for 16 hr. After the polymerization, the vial was immediately chilled in an ice-bath and opened to air to prevent further polymerization. A sample of the crude solution was taken for NMR to determine the conversion of the monomer(s). The polymer was the precipitated from MeOH and dried for at least 4 hr. The procedure was performed an additional two times. The polymer was placed under high vacuum (~ 40 mTorr) for 72 hr prior to further evaluation. The dried polymer was subjected to NMR and SEC to determine final polymer composition, number average molecular weight, and dispersity (Fig. S1-S8, Table S1).

To synthesize polymers with varying HEMA composition, similar polymerization techniques were used compared to the styrene homopolymer synthesis. The total amount of monomer added was kept constant at 120 mmol, but the feed ratio for Styrene and HEMA was varied. Individual polymerizations were carried using monomer feed ratios found in Table 1. All HEMA copolymers were precipitated in methanol except for the 31.2% HEMA copolymer which was precipitated in hexane. DMF was used as the solvent for the copolymerization due to the previously reported similarity in the reactivity ratios (r_{ST} = 0.53, r_{HEMA} = 0.59)[12]. These values minimize compositional drift during the polymerization process and ensured the initial feed ratio of HEMA closely related to the incorporation in the final copolymer. It is worth noting that the polymer with 31.2% HEMA incorporation did not yield a stable polymer. After a year stored under ambient conditions, the polymer became insoluble and could not be processed or accurately analyzed by GPC (Fig. S2).

Table 1: Monomer feed ratios used for polymerization of styrene and HEMA.

	Styrene (mL, g, mmol, eq)	**HEMA (mL, g, mmol, eq)**	**% HEMA***
A	13.8 mL, 12.5 g, 120 mmol, 500 eq	0 mL, 0 g, 0 mmol, 0 eq	0.0 %
B	13.4 mL, 12.2 g, 117 mmol, 487.5 eq	0.36 mL, 0.39 g, 3 mmol, 12.5 eq	3.0 %
C	13.1 mL, 11.9 g, 114 mmol, 475 eq	0.98 mL, 1.05 g, 6 mmol, 25 eq	7.7 %
D	12.6 mL, 11.4 g, 109.8 mmol, 457.5 eq	1.24 mL, 1.37 g, 10.2 mmol, 42.5 eq	11.5 %
E	11.6 mL, 10.6 g, 101.4 mol, 422.5 eq	2.25 mL, 2.24 g, 18.6 mmol, 77.5 eq	20.2 %
F	10.0 mL, 9.0 g, 87 mmol, 362.5 eq	4.00 mL, 4.29 g, 33 mmol, 137.5 eq	31.2 %

* Determined via NMR of precipitated and dried NMR

^{1}H NMR spectroscopy was conducted using Bruker Advance 400 MHz or 500 MHz instruments. Polymer samples were analyzed using a Tosoh EcoSEC HLC 8320GPC system with TSKgel SuperHZ-L columns eluting $CHCl_3$ containing 0.25% NEt_3 at a flow rate of 0.45 mL/min. Initial number-average molecular weights (M_n) and dispersities ($Đ$) were calculated from refractive index chromatograms using PStQuick Mp-M polystyrene standards. Unless otherwise stated, reported M_n

and *Đ* were obtained from multi-angle light scattering (MALS), Wyatt 8-angle measured with complete elution was used. 100% mass recovery was assumed to calculate M_n.

Copolymer Thin Film Preparation

Polymer films were prepared via spin-coating from chloroform solutions. Film thickness was chosen to (1) be sufficiently thick to avoid effects on T_g due to interactions with the substrate or free surface and (2) be sufficiently thin to be fully infiltrated via VPI within a reasonable amount of time. We find that a thickness of about 200 nm met both of these criteria for our PS-*r*-PHEMA thin films. Ellipsometry-measured T_g for 170 nm films and 200 nm films remains constant at 100˚C, and second ion mass spectrometry (SIMS) of VPI-treated films indicated that most copolymers were fully infiltrated (S14).

To achieve this thickness, each copolymer was dissolved in chloroform at a ratio of about 2 wt% polymer content. Pure polystyrene was dissolved in toluene at 5 wt%. Solutions were stirred for at least 24 hr and sat at rest for at least another 24 hr, letting any contaminants settle. Silicon wafers cut into 1 x 1 in^2 pieces were air plasma cleaned for 1 min in an 18 W RF PDC-001-HP Plasma Cleaner to remove organic contaminates. Tiles were then spun cast at 3000 rpm for 60 s (SCS 6800 spin coater). At about 5 s into the spin cycle, about 1 mL of polymer solution was dropped onto the spinning silicon wafer. After spin-coating, polymer thin films were heated on a hot plate at 150°C for at least 1 hr to fully relax the films.

Vapor Phase Infiltration

Fig. 1 shows the sequencing used to vapor phase infiltrate the PS-*r*-PHEMA thin films with AlO_x. VPI was carried out at 100 °C in a custom-built VPI reactor. All dose sequencing was done with a tree-based LabVIEW software code[13]. An initial 1 hr purge (pulling 30 mTorr vacuum and then flowing 99.99+% nitrogen at 1 Torr) removed water from the films and reaction chamber. After pulling vacuum (~30 mTorr) for an additional 5 min and isolating the chamber for 2 min, TMA was dosed from a room temperature source through a 0.27 flow coefficient (C_v) valve for 5 s into a 0.028 m^3 chamber to achieve a 0.5 torr partial pressure of TMA, held in the chamber for 4 hr, and finally purged with 1 Torr nitrogen for 2 hr. After another 5 min pump down and 2 min isolation, water was dosed (from room temperature through a similar valve for 5 s to give 1.5 Torr partial pressure H_2O), held, and purged for the same time intervals as TMA.

VPI reaction parameters were selected to be well in excess of what is needed to achieve complete saturation of the polymer film based on a prior kinetics study conducted with PS-*r*-PHEA (HEA standing for hydroxyl ethyl acrylate), a chemically similar copolymer to PS-*r*-PHEMA (Fig. S9). Swelling data in Figure S9 indicates minimal volumetric changes in copolymer films between 1 min and 1000 min purge times, suggesting that most unbound TMA leaves the copolymer within the first

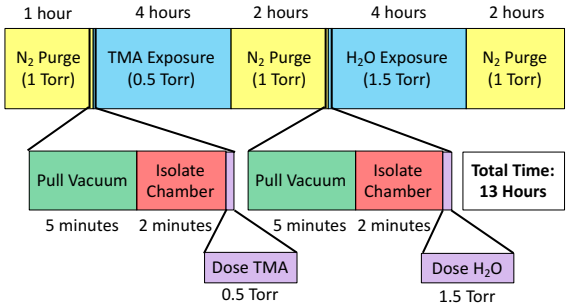

Figure 1: Schematic depiction of vapor phase infiltration procedure.

---

min of nitrogen purging. 2 hr purges were chosen for PS-*r*-PHEMA studied in this investigation to minimize the presence of unbound alumina in the polymer. SIMS data in Fig S10 confirms that most copolymers were fully infiltrated with our selected TMA hold time of 4 hr.

Spectroscopic Ellipsometry & Measurement of Glass Transition Temperatures

Thin film thicknesses were measured using a J.A. Woollam alpha-SE Ellipsometer retrofitted with a custom-built heating stage (Fig. S11). Thickness and refractive index (RI) analysis was done using CompleteEASE software. We designed a Cauchy model to represent the copolymer and VPI hybrid films, fitting A, B, and k Cauchy coefficients for refractive index in addition to thickness. This layer was stacked on top of a 1.7 nm layer of native SiO_2 and a silicon substrate.

Copolymer thickness and RI for copolymers were measured at 60°C (using the ellipsometer's hot plate) before and after vapor phase infiltration. These measurements were always taken within 0.5 hr after 150°C heat treatments, to minimize water sorption into the films, which might conflate thickness results. We measured the same spot on each film before and after VPI to the best of our ability, minimizing variation from heterogeneous spin-coating across the film (i.e. films were thicker near the edges, so measurements were taken at the center).

Glass transition and coefficients of thermal expansion were determined by measuring copolymer thickness over a temperature ramp. Measurements were taken at 5 °C intervals, holding the films at each temperature for approximately 10 s. Differences in measured thermal expansions and T_g values between films measured at 10 s and 30 s hold times were negligible, so 10 s holds appear sufficient for thermal equilibrium (Fig. S12). Films remained stationary throughout each temperature excursion such that the exact spot was continuously measured.

Polymer was removed from the hybrid material via 1 hr of plasma cleaning, and the remaining AlO_x was sintered in a furnace at 700°C for 1 hr in order to reduce its porosity. Alumina thicknesses were measured via ellipsometry using a Cauchy model with fixed RI constants (RI fitting becomes unrealistic below 50 nm).

Submersion of Hybrid Films in Chloroform

In separate experiments, 200 nm VPI-treated PS-*r*-PHEMA films were submerged in separate containers, each with 10 ml chloroform, a good solvent for the pure copolymer. Thin film thicknesses were measured before submersion, and after 1, 3, 10, and 30 hr in chloroform. After each submersion interval, the films were removed from solution and held against Kimwipes to remove chloroform from the surface. Film thicknesses were then measured on an ellipsometer after no longer than 10 min outside of solution to capture any swelling phenomena in addition to film dissolution. Films were returned to their original solutions for continued exposure. After the 30-hr measurement, films were heated to 150°C for 1 hr in ambient to remove any solvent or swelling and measured once more. This experiment was repeated for untreated copolymers, dissolving them for 1 hr.

Fourier-Transform Infrared Spectroscopy (FTIR)

FTIR spectra were measured using a Thermo Fisher Scientific Nicolet iS5 Spectrometer with an iD7 ATR and an AR-coated diamond crystal. Through OMNIC software, absorption spectra were collected with 2 cm^{-1} resolution and 128 scans per copolymer. We drop-casted micron-thick copolymers onto silica glass slides for FTIR to reduce noise on the spectra. As with spin-coated films, the drop-casted films were dried and annealed at 150°C on a hot plate, but for 3 hr. due to their larger thickness. FTIR spectra were collected for each copolymer before and after vapor phase infiltration.

Secondary-Ion Mass Spectrometry (SIMS)

SIMS spectra of the 200 nm AlO_x-PS-*r*-PHEMA films were measured with an IONTOF 5-300 Time-of-Flight SIMS system. A 2 keV Cs^+ ion beam was focused onto a 150x150 μm square section of the VPI-treated 200 nm PS-*r*-PHEMA films, and a 50x50 μm section within this region was analyzed. The beams penetrated through polymer films and into the silicon substrate after 300 s of ion beam analysis.

RESULTS AND DISCUSSION

Alumina Uptake in Copolymer Films

Fig. 2 presents three ellipsometry-based metrics that relate VPI alumina loading with initial copolymer composition: copolymer film swelling, pyrolyzed alumina thickness, and alumina mass uptake. Film swelling is the change in film thickness before and after VPI. Hybrid films were then plasma treated and pyrolyzed to remove the organic and reduce porosity. The remaining aluminum oxide (alumina) film thickness was then measured. The residual alumina films fit well (a mean square error of less than 5) to a Cauchy model with a fixed refractive index of 1.660, matching well to literature values for amorphous alumina[14]. An inorganic mass uptake is also estimated using these film thicknesses and assuming material densities:

$$w_{AlO_x} = \frac{V_{AlO_x} * \rho_{AlO_x}}{V_{PS-PHEMA} * \rho_{PS-PHEMA}} \quad (1)$$

Where w_{AlOx} is the percent increase in film mass via inorganic uptake, V_{AlOx} is film swelling, $V_{PS\text{-}r\text{-}PHEMA}$ is original film thickness (assuming volume and thickness are proportional), and ρ is density for alumina and copolymer, respectively. Copolymer density is assumed to fit a linear interpolation between pure PS (1.05 g/ml)[15] and PHEMA (1.15 g/ml)[16]. Amorphous alumina density of 3.2 g/ml is based on the literature value for atomic layer deposited (ALD) amorphous alumina films[17]. The physical thicknesses of the initial polymer films varied by up to 20 nm depending, but this variation becomes normalized in the form of wt.% mass uptake. As a secondary reference, we also plot in the inset the percent increase in film thickness after VPI.

Fig. 2 demonstrates that all three of these metrics indicate a monotonic increase in inorganic loading with increase concentration of HEMA units in the polymer. Increasing alumina uptake with HEMA content supports the expectation that polymer-VPI reactivity can be controlled by the concentration of reactive groups in the polymer. HEMA's hydroxyl group (and possibly its carbonyl group) are reactive toward TMA, while styrene should have near-zero reactivity toward TMA[18, 19, 20]. Film swelling ranges from 1.2 nm (0.56 vol.%) in pure polystyrene (0% HEMA) to 14.4 nm (6.5 vol.%) in 20.2 mol.% HEMA. Pyrolyzed alumina thickness ranges from 2.3 to 12.5 nm, and mass uptakes from 3.2 wt.% to 17.0 wt.%. These increases are approximately linearly up to about 12 mol% HEMA. However, the amount of inorganic loading appears to slow at ca. 20 mol% HEMA. SIMS data collected from these 20 mol% HEMA films (Fig. S10) indicates that the concentration of inorganic alumina loading is high near the surface and does not fully load into the entire depth of the film. This structure suggests that these high concentration HEMA copolymers are highly reactive toward TMA, leading to the formation of a dense inorganic loading near the surface that restricts subsequent sorption and diffusion of TMA into the bulk of the film, limiting total mass uptake. Thus, these 20 mol% HEMA hybrids are heterogeneous in their composition with film depth. Partial infiltration for this copolymer composition also likely explains its deviation from the VPI-T_g trend

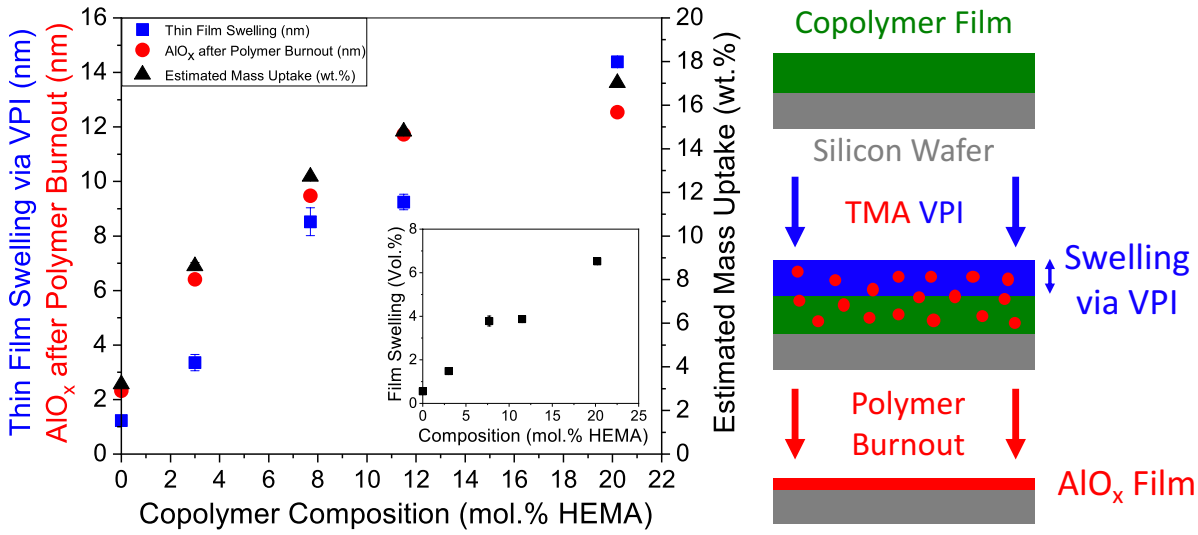

Figure 2: A plot of four metrics for alumina uptake after VPI of PS-r-PHEMA copolymer films as a function of chemistry (mol% HEMA). (1) Change in thin film thickness (i.e., "swelling") upon VPI (blue squares), (2) total inorganic film thickness after burning off polymer (red circles), (3) wt.% alumina (black triangles) calculated from the (1) and (2) measured thicknesses, and percent film swelling based on (1) (black squares in inset) all as a function of copolymer composition. Image to the right depicts these thicknesses.

discussed in the next section. Both phenomena – linear increases at low reactivity and reduced diffusivity at high reactivity – are supported in principal by similar behavior in VPI-treated PS-r-PMMA random copolymers, as reported by Perego et al[20].

Ellipsometry measurements show refractive indices of PS-*r*-PHEMA films vary from 1.597 (pure PS) to 1.575 (copolymer with 20.2% HEMA) ± 0.001 at 500 nm (Fig. S13). This range is consistent with literature values for pure polystyrene (1.604 at 500nm)[21] and poly(hydroxyethyl methacrylate) (1.51)[22]. The refractive indices do not change very much after VPI (Fig. S13). The largest change is an increase of only 0.006 ± 0.002 for the 7.7 mol% HEMA composition. While the refractive index of crystalline sapphire is above 1.7, the refractive index of amorphous ALD alumina is typically between 1.60 and 1.65[23], near that of the polymer. Thus, the observed subtle change in refractive index is consistent with expectations for loading this polymer with a few percent of amorphous inorganic alumina.

Finally, it is interesting to note that the pyrolyzed alumina film thicknesses in Fig. 2 (red circles) exceed the amount of film swelling (blue squares) measured for the hybrid material at all low HEMA concentrations (< 14 mol%). This larger thickness for the pyrolyzed inorganic suggests that a portion of the inorganic in the hybrid structure is filling what was previously free volume and not contributing to a volume change in the hybrid, i.e., not "swelling" the polymer. An alternative explanation is that pyrolyzing the films also grows a few nm of SiO_2 beneath the alumina layer. At this point, it is difficult

to ascertain which explanation is correct, but this trend along with the changes in refractive index do merit further investigation to better understand the changes to the physicochemical structure of these materials upon infiltration.

Thermal Expansion and Glass Transition

Fig. 3 plots the temperature dependent film thickness of both the copolymer and VPI hybrids for each of these copolymer compositions. The linear slopes in these thickness-vs-temperature plots are the coefficients of thermal expansion (CTEs) for each of these films (measured CTEs are plotted in Fig. S14). The abrupt changes in these slopes with temperature indicate the glass transition in these materials. We have used the graphical intersection of these slopes to determine T_g. These lines were fitted with least squares regression, using all data points except those nearest T_g (because some temperature ramps show a gradual transition between the two regimes of thermal expansion). Error bars in Fig. 3 (a-e) represent three films of each copolymer measured before and after infiltration. Error bars in Fig. 3 (f) were estimated using the intersections of 95% confidence bands for the regressions shown in Fig. 3 (a-e).

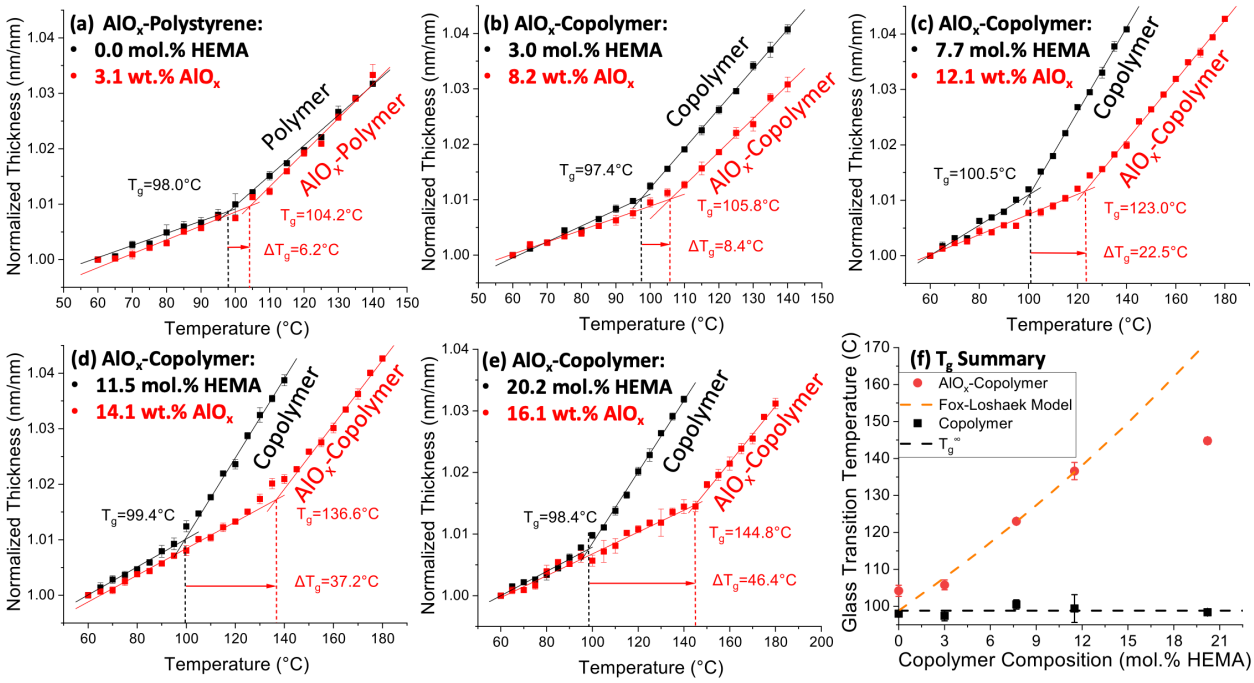

Figure 3: (a-e) Normalized thin film thickness of untreated PS-r-PHEMA (black) and vapor phase infiltrated AlO_x-PS-r-PHEMA (red) vs film temperature for various copolymer compositions: (1) 0 mol% HEMA, (b) 3 mol% HEMA, (c) 7.7 mol% HEMA, (d) 11.5 mol% HEMA, (e) 20.2 mol% HEMA. (f) Glass transition temperature of untreated copolymer (black) and vapor phase infiltrated AlO_x-PS-r-PHEMA hybrids (red) as a function of polymer composition. Orange dashed line is a fit to the Fox-Loshaek crosslink theory, assuming every HEMA unit is crosslinked. Black dotted line shows T_g^{∞}, average glass transition temperature of all copolymers pre-VPI treatment. Some error bars are obscured by data points.

In all cases, T_g increases after VPI transforms the polymer into a hybrid material. T_g also shows a remarkably clear increase with increasing inorganic loading concentration. Fig. 3 (f) summarizes T_g values for untreated copolymers and AlO_x-PS-*r*-PHEMA hybrids. T_g for untreated PS-*r*-PHEMA copolymers remains within 3 °C of the literature value for T_g of pure polystyrene, 100°C[24]. After VPI processing, T_g values for AlO_x-PS-*r*-PHEMA start at 104°C for AlO_x-PS (0 mol.% HEMA and 3.1 wt.% alumina) and increases up to 145°C for the most infiltrated PS-*r*-PHEMA (20.2 mol.% HEMA, 16.1 wt.% alumina). Because HEMA content is related to alumina content at low HEMA compositions, this trend suggests that increasing vapor-phase-infiltrated alumina content in PS-*r*-PHEMA films suppresses chain mobility, raising T_g.

Interestingly, the T_g of PS-*r*-PHEMA before VPI treatment did not change with HEMA composition, remaining constant at 98.9˚C ± 0.7˚C. While most literature values for the T_g of pure PHEMA are reported near 80˚C, some authors have measured T_g's for this homopolymer as high as 115˚C, which may be the result of mild crosslinking in ambient humidity[25, 26, 27]. Accordingly, it is possible that our copolymers were mildly crosslinked before VPI treatment, offsetting any plasticizing effects from PHEMA. However, these pure PS-r-PHEMA films still readily dissolved in chloroform, indicating that any cross-linking was very minimal.

The formation of O-Al-O crosslinks between PS-*r*-PHEMA chains is one possible explanation for the increase in T_g with inorganic loading concentration. Alternative mechanisms include (i) a reduction in free volume as small AlO_x molecules occupy space between polymer chains or (ii) intermolecular attraction between alumina and polymer hydroxyls, both reducing chain mobility[28,29]. However, the possibility of chemical cross-link formation is uniquely supported by dissolution results discussed in the subsequent section. The Fox-Loshaek equation[30] (2) modelling T_g and crosslinking density (X_c) for large linear polymers crosslinked post-synthesis is fitted to the data in Fig. 6f and presented here (simplified by Stutz *et al.*[9]):

$$T_g = T_g^{\infty}\left(1 + K_2\frac{X_c}{1-X_c}\right) \quad (2)$$

Here, K_2 is a material constant describing the impact the specific crosslinker chemistry has on T_g. This model only accounts for changes in T_g as a function of crosslinks, so T_g^{∞} is defined as the average glass transition temperature of all copolymers before VPI-treatment (98.8°C). Assuming all HEMA units are crosslinked, X_c is equivalent to the mole fraction of HEMA units. This fit is shown as the dashed orange line in Fig. 3f. Pure polystyrene is excluded from this model because the PS likely does not form significant chemical bonds with TMA and thus the change in glass transition temperature may be due to another mechanism, like unbound inorganic clusters impeding micro-Brownian or segmental motion of polymer chains. The copolymer with 20.2 mol.% HEMA is also excluded because it is not fully infiltrated. In fact, the supposition that this polymer is only partially infiltrated (not all of the hydroxyls have been reacted into crosslinks) is further supported

by the observation that T_g for 20.2 mol.% HEMA VPI-treated polymer lies below the predicted Fox-Loshaek value for that composition.

Because the Fox-Loshaek model takes a linear form at low crosslink density, K_2 can be thought of as the slope of T_g vs. X_c, or in other words, the extent to which a crosslinker reduces chain mobility. Here, we find a K_2 value of 3.0 ± 0.1 for these hybrid materials. This value is more than 3 times larger than the K_2 values for conventional crosslinked polymers, such as ethyleneglycoldimethacrylate with methyl methacrylate, divinylbenzene with styrene, and polyurethane, which have K_2 values of 0.92, 0.775, and 0.93 respectively[9]. One possible explanation is that these inorganic crosslinks are "stiffer" bonds than conventional organic crosslinks. Alternatively, the unusually high K_2 value could indicate that many polymer chains are being crosslinked at each inorganic site. VPI of TMA + H_2O is believed to potentially form inorganic clusters upon reaction within the polymer[31]. These clusters should be covalently bound to the copolymer chains and through condensation reactions could further aggregates to form high-functionality crosslinks with effectively high K_2 values. Irrespective of the exact mechanism, these observations suggest that VPI has the potential to more effectively reduce the polymer chain mobility than conventional crosslinker chemistries. While we recognize this initial evaluation is based upon fitting this theory to only 3 measured values and makes several underlying assumptions, we do believe these results to be noteworthy and of merit for further exploration in subsequent studies. Specifically, it should be noted that out assumption that the concentration of cross-links (X_c) is the total concentration of HEMA units is likely a conservative assumption for calculating K_2. If less HEMA units are cross-linked, then K_2 would be even larger than what we report here.

Chemical Stability and Swelling of Hybrid Films

Enhanced resistance to chemical dissolution can provide further evidence for the cross-linked structure of these AlO_x-PS-*r*-PHEMA hybrid materials[32]. Fig. 4 presents an *ex situ* submersion study of AlO_x-PS-*r*-PHEMA hybrid films in chloroform. All untreated polymers dissolved in chloroform within 1 hr of submersion. VPI infiltrated AlO_x-PS (0 mol.% HEMA) thin films also drop from about 200 nm in thickness to below 10 nm within the first hour of chloroform exposure, suggesting these materials are also largely susceptible to dissolution chloroform. In contrast, all of the hybrid AlO_x-copolymers maintained full film thickness upon immersion in chloroform, suggesting a resistance to dissolution. In fact, all of the hybrid copolymer films showed a modest increase in thickness, which is attributed to the behavior of a cross-linked polymer "swelling" in a good solvent. To test this hypothesis, after 30 hr of immersion in chloroform, these presumably swollen hybrid films were heated for 1 hr at 150°C in air to remove any sorbed solvent. In all cases upon heating, the film thickness

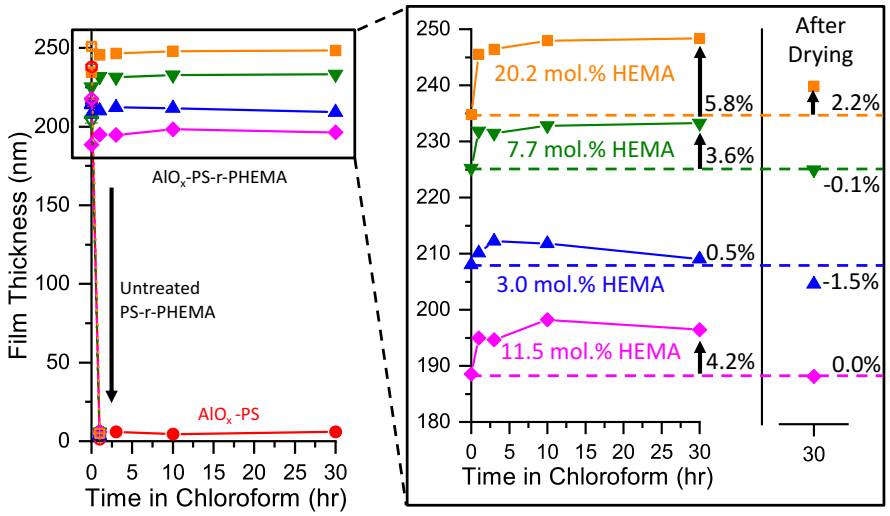

Figure 4: (Left) Film thicknesses of untreated PS-r-PHEMA copolymer films (dashed lines, hollow shapes) and VPI-treated hybrid films (solid lines, filled shapes) as a function of immersion time in chloroform. Untreated films fully dissolved after 1 hour (no data shown beyond 1 hr). (Right) A magnified region of the AlO_x-PS-r-PHEMA hybrid film thicknesses is included for clarity. Beside this magnified region is a separate series of thicknesses showing the change in thickness after films that were immersed for 30 hrs were then dried at 150°C for 1 hour in ambient on a hot plate. Dashed lines in this magnified plot show the original film thickness prior to chloroform immersion with percent increase or decrease after 30 hrs of immersion and after drying.

contracts to within 2.2% of its original thickness prior to chloroform exposure, providing further evidence that the thickness increase was indicative of the chloroform solvent swelling the film.

While higher degrees of crosslinking would be expected to reduce the extent of swelling, this trend is not fully held in the magnified plot shown on the right side of Fig. 4. Specifically, the low inorganic loading, 3 mol.% HEMA swelled by 0.5% of its original thickness after 30 hr, compared to 5.8% swelling for 20.2 mol.% HEMA. We speculate that this result indicates partial dissolution of this film, which is acting in opposition to potential film swelling. In fact, over the time period studies, the dissolution data shows a moderate downward trend with dissolution time and the final thickness after drying is markedly lower (1.5%) than the initial thickness, both of which suggest partial dissolution for this lowest HEMA concentration film. Thus, copolymer concentrations of greater than 3 mol% HEMA are likely needed to make hybrid films that are fully resistant to chemical dissolution for this particular VPI chemistry and process condition.

Chemical Bonding Between Alumina and PS-*r*-PHEMA

In general, we believe that during TMA dosing and holding, TMA undergoes a substitution reaction with the hydroxyl groups in PS-*r*-PHEMA, binding aluminum to the polymer with a C-O-Al bond and releasing methane (Fig. 5). During the water dose-and-hold, hydroxyl bonds replace all remaining Al-methyl bonds, releasing more methane. By bonding to multiple chains during the first step, TMA may form crosslinks that significantly alter material properties. It is also possible

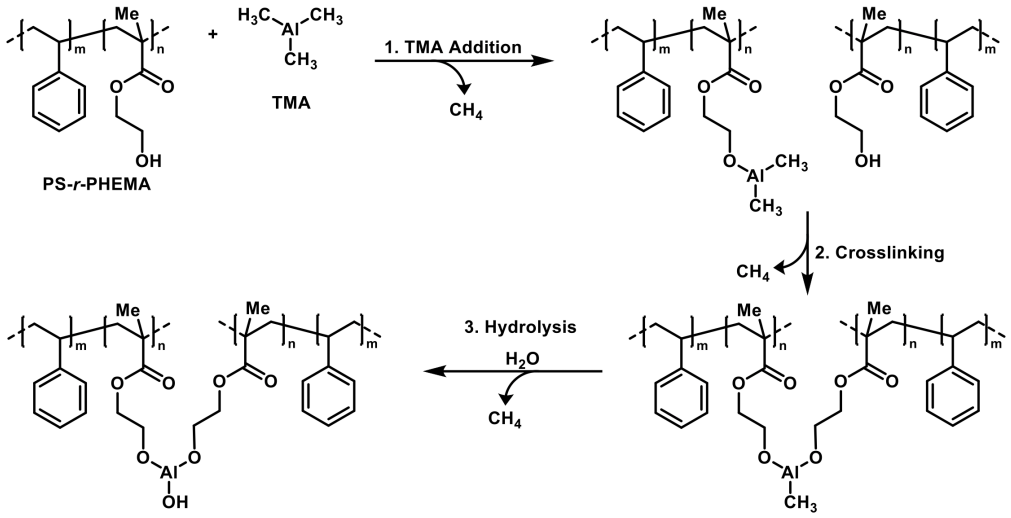

Figure 5: Proposed chemical reactions between PS-*r*-PHEMA, TMA, and water during VPI.

that the final hydroxylated aluminum groups could undergo condensation reactions with one another forming additional crosslinks.

While TMA is known to react with both carbonyl and hydroxyl groups within a polymer[33, 34], we believe that at the processing conditions and chemistries used here, TMA most likely reacts first with PHEMA's hydroxyl groups before possible associations or reactions with the carbonyl groups. Previous literature suggests that carbonyl-TMA bonds are reversible at the process temperature used here (100 °C) and the associated complex that forms dissociates once the TMA reacts with water[32, 34]. By comparison, DFT calculations predict that TMA will exothermically react with and form permanent covalent bonds to hydroxyl functional groups on organic molecules[35]. Such primary chemical bonds are likely needed to make the hybrid material insoluble in chloroform as observed. We have also observed TMA diffusion to be more impeded in PS-*r*-PHEMA than in PMMA, which only has carbonyl groups[36]. In fact, at 20% HEMA, the films studied here can no longer be fully infiltrated. This suggests a higher reaction rate than with polymers like PMMA that only contain carbonyl groups. Overall, these observations strongly suggest that the TMA reacts more readily with the PHEMA's hydroxyl groups than its carbonyl groups.

FTIR spectra were collected in an attempt to identify chemical bonds between alumina and PS-*r*-PHEMA (Fig. 6). The intensity of each spectra for AlO_x-copolymers (i.e. after VPI) is normalized to match the equivalent untreated methylene stretch of the copolymer (before VPI) at 2930 cm^{-1}, which is not expected to change. This peak represents C-H bending in the methylene polymer backbone, which exists at a significant composition in all PS-*r*-PHEMA copolymers tested. All other

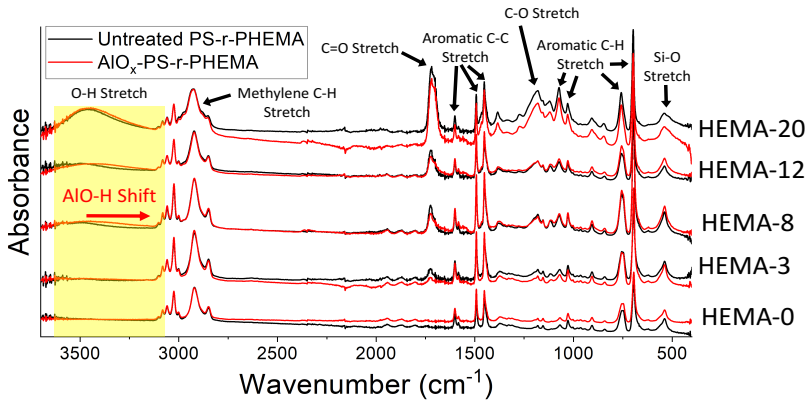

Figure 6: Fourier-Transform Infrared Spectra (FTIR) of PS-*r*-PHEMA copolymers before and after vapor phase infiltration.

peaks in the spectra can be matched to the aromatic bonds in styrene, the C=O, C-O, and O-H bonds in HEMA, and the Si-O bonds in the wafer. Peak-by-peak assignment is included in the S.I.

Only one notable difference in FTIR spectra emerges from VPI treatment: a broadening and blue shift of the hydroxyl stretch at from 3300 to 3500 cm^{-1}. This shift may reflect hydroxyls in a different chemical environment than the HEMA units, such as those bonded to inorganic alumina species. Alternatively, VPI treatment may have affected the hydrophobicity of the films, resulting in more or less water sorption. To minimize this latter effect, FTIR was taken within 15 min after 1-hr heat treatments at 150°C, so we do not believe this to be a significant contribution.

Other than this shift, no FTIR peaks are noticeably shifted, formed, removed, amplified, or reduced as a result of vapor phase infiltration. Accordingly, these results suggest that alumina may be (a) chemically unbound to the copolymers, thereby showing no organic-inorganic bonds, (b) bound in a manner that does not appear in FTIR spectra, or (c) bound in a manner that does not change the stoichiometric proportions of chemical bonds. Some possible chemical reactions between alumina, PS-*r*-PHEMA and water are further discussed in the S.I.

While we are unable to detect clear spectroscopic evidence for the structure proposed in Figure 5, we still believe the chemical and thermophysical properties observed, including an increase in T_g and enhanced resistance to chemical dissolution support the conclusion of chemical cross-linking in these hybrid materials. While the exact structures of these hybrids remain an open question for the community, the results presented here provide new insights into the thermophysical properties that are possible with these materials.

CONCLUSIONS

Herein we reported vapor phase infiltration's ability to transform a polymer into an organic-inorganic hybrid material with a T_g that is tens of degrees Celsius higher than the parent polymer. For the specific system of study—PS-*r*-PHEMA copolymers infiltrated with AlO_x via a TMA + H_2O chemistry—linearity between the copolymer's HEMA content, volumetric swelling after VPI, and residual inorganic film thickness after pyrolysis confirms that the concentration of alumina in the hybrid material is directly related to the concentration of copolymer constituent (HEMA) reactive toward the VPI precursors (TMA). Of the copolymers tested that were known to be homogeneously infiltrated throughout the entire film thickness, PS-*r*-PHEMA with 11.5 mol.% HEMA exhibited the largest shift in T_g upon infiltration, 37.2 °C (from 99.4˚C to 136.6˚C). Increasing T_g with increasing alumina content suggests that inorganic units are serving as crosslinks within the copolymer, and the T_g data fits well to the Fox-Loshaek model with a K_2 constant 3x higher than what is expected for most organic cross-links. While chemical bonding between alumina and PS-*r*-PHEMA could not be detected with FTIR, the supposition that crosslinks are formed by this VPI process is supported by the resistance of infiltrated films to chemical dissolution in a solvent that readily dissolves the parent polymer. In summary, these results demonstrate that VPI can be used to alter the thermophysical properties of polymers, opening new opportunities for increasing the thermal stability of polymer coatings, fibers, fabrics, foams, and membranes.

ASSOCIATED CONTENT

Supporting Information

The Supporting Information is available free of charge on the ACS Publications website.

Retrofitted ellipsometer; SEC and NMR for PS-*r*-PHEMA; VPI purge length experimental results; heated ellipsometry thermal equilibration experimental results; refractive indices and thermal expansivity for PS-*r*-PHEMA and AlO_x- PS-*r*-PHEMA; SIMS for AlO_x- PS-*r*-PHEMA (PDF)

AUTHOR INFORMATION

Corresponding Authors

*Email: will.gute@chemistry.gatech.edu (W.R.G.)

*Email: losego@gatech.edu (M.D.L)

Author Contributions

The manuscript was written through contribution of all authors. All authors have given approval to the final version of the manuscript.

Notes

The authors declare no competing financial interest.

ACKNOWLEDGMENTS

J.T.B. was supported by Georgia Tech's President's Undergraduate Research Award funding and the Roxanne D. Westendorf Undergraduate Research Fund. C.Z.L. was supported by the American Chemical Society Petroleum Research Fund under Grant # 55526-DNI10. R.A.L was supported by the American Chemical Society Petroleum Research Fund under Grant # 59312-DNI7. Furthermore, we are thankful for the generous support of this project by the Department of Education Graduate Assistance in Areas of National Need (GAANN) program at Georgia Institute of Technology (Award #P200A180075). Materials and research support funding was partially supplied by the National Science Foundation (DMREF-1921873). This work was performed in part at the Georgia Tech Institute for Electronics and Nanotechnology, a member of the National Nanotechnology Coordinated Infrastructure (NNCI), which is supported by the National Science Foundation (ECCS-2025462).

REFERENCES

1. Barry, E.; Mane, A. U.; Libera, J. A.; Elam, J. W.; Darling, S. B., Advanced oil sorbents using sequential infiltration synthesis. *J. Mater. Chem. A Mater. Energy Sustain.* **2017,** *5* (6), 2929-2935.

2. Deckman, I.; Moshonov, M.; Obuchovsky, S.; Brener, R.; Frey, G. L., Spontaneous interlayer formation in OPVs by additive migration due to additive–metal interactions. *J. Mater. Chem. A Mater. Energy Sustain.* **2014,** *2* (39), 16746-16754.

3. Tseng, Y.-C.; Peng, Q.; Ocola, L. E.; Czaplewski, D. A.; Elam, J. W.; Darling, S. B., Etch properties of resists modified by sequential infiltration synthesis. *J. Vac. Sci. Technol. B Nanotechnol. Microelectron.* **2011,** *29* (6), 06FG01.

4. Berman, D.; Guha, S.; Lee, B.; Elam, J. W.; Darling, S. B.; Shevchenko, E. V., Sequential infiltration synthesis for the design of low refractive index surface coatings with controllable thickness. *ACS Nano* **2017,** *11* (3), 2521-2530.

5. McGuinness, E. K.; Zhang, F.; Ma, Y.; Lively, R. P.; Losego, M. D., Vapor phase infiltration of metal oxides into nanoporous polymers for organic solvent separation membranes. *Chem. Mater.* **2019,** *31* (15), 5509-5518.

6. Bandzierz, K.; Reuvekamp, L.; Dryzek, J.; Dierkes, W.; Blume, A.; Bielinski, D., Influence of network structure on glass transition temperature of elastomers. *Materials (Basel)* **2016,** *9* (7), 607.

7. DiMarzio, E. A., On the second-order transition of a rubber. *J. Res. Natl. Bur. Stand. A Phys. Chem.* **1964,** *68A* (6), 611-617.

8. Jin, K.; Torkelson, J. M., Enhanced tg-confinement effect in cross-linked polystyrene compared to its linear precursor: Roles of fragility and chain architecture. *Macromolecules* **2016,** *49* (14), 5092-5103.

9. Stutz, H.; Illers, K. H.; Mertes, J., A generalized theory for the glass transition temperature of crosslinked and uncrosslinked polymers. *J. Polym. Sci. B Polym. Phys.* **1990,** *28* (9), 1483-1498.

10. Rubinstein, M.; Colby, R. H., *Polymer Physics*. Oxford University Press: London, England, 2003.

11. Painter, P. C.; Coleman, M. M., *Essentials of polymer science and engineering*. DEStech Publications: Lancaster, CA, 2008.

12. Lebduska, J.; Snuparek, J.; Kaspar, K.; Cermak, V., Solution Copolymerization of Styrene and 2-Hydroxyethyl Mechacrylate. *J Polym Sci Pol Chem* **1986,** *24* (4), 777-791.

13. Piercy, B. D.; Losego, M. D., Tree-based control software for multilevel sequencing in thin film deposition applications. *J. Vac. Sci. Technol. B* **2015,** *33* (4), 5.

14. Nayar, P.; Khanna, A.; Kabiraj, D.; Abhilash, S. R.; Beake, B. D.; Losset, Y.; Chen, B., Structural, optical and mechanical properties of amorphous and crystalline alumina thin films. *Thin Solid Films* **2014,** *568*, 19-24.

15. Sharp, D. G.; Beard, J. W., Size and Density of Polystyrene Particles Measured by Ultracentrifugation. *J Biol Chem* **1950,** *185* (1), 247-253.

16. Poly(2-hydroxyethyl methacrylate). https://www.sigmaaldrich.com/catalog/product/sigma/p3932?lang=en&region=US.

17. DeCoster, M. E.; Meyer, K. E.; Piercy, B. D.; Gaskins, J. T.; Donovan, B. F.; Giri, A.; Strnad, N. A.; Potrepka, D. M.; Wilson, A. A.; Losego, M. D.; Hopkins, P. E., Density and size effects on the thermal conductivity of atomic layer deposited TiO2 and Al2O3 thin films. *Thin Solid Films* **2018,** *650*, 71-77.

18. Peng, Q.; Tseng, Y. C.; Long, Y.; Mane, A. U.; DiDona, S.; Darling, S. B.; Elam, J. W., Effect of Nanostructured Domains in Self-Assembled Block Copolymer Films on Sequential Infiltration Synthesis. *Langmuir* **2017,** *33* (46), 13214-13223.

19. Segal-Peretz, T.; Winterstein, J.; Doxastakis, M.; Ramirez-Hernandez, A.; Biswas, M.; Ren, J. X.; Suh, H. S.; Darling, S. B.; Liddle, J. A.; Elam, J. W.; de Pablo, J. J.; Zaluzec, N. J.; Nealey, P. F., Characterizing the Three-Dimensional Structure of Block Copolymers via Sequential Infiltration Synthesis and Scanning Transmission Electron Tomography. *Acs Nano* **2015,** *9* (5), 5333-5347.

20. Caligiore, F. E.; Nazzari, D.; Cianci, E.; Sparnacci, K.; Laus, M.; Perego, M.; Seguini, G., Effect of the Density of Reactive Sites in P(S-r-MMA) Film during Al2O3 Growth by Sequential Infiltration Synthesis. *Advanced Materials Interfaces* **2019,** *6* (12).

21. Sultanova, N.; Kasarova, S.; Nikolov, I., Dispersion properties of optical polymers. *Acta Phys. Pol. A.* **2009,** *116* (4), 585-587.

22. Karaman, M.; Kooi, S. E.; Gleason, K. K., Vapor deposition of hybrid organic–inorganic dielectric Bragg mirrors having rapid and reversibly tunable optical reflectance. *Chem. Mater.* **2008,** *20* (6), 2262-2267.

23. Gorham, C. S.; Gaskins, J. T.; Parsons, G. N.; Losego, M. D.; Hopkins, P. E., Density dependence of the room temperature thermal conductivity of atomic layer deposition-grown amorphous alumina (Al2O3). *Appl. Phys. Lett.* **2014,** *104* (25).

24. Kim, S.; Hewlett, S. A.; Roth, C. B.; Torkelson, J. M., Confinement effects on glass transition temperature, transition breadth, and expansivity: comparison of ellipsometry and fluorescence measurements on polystyrene films. *Eur. Phys. J. E Soft Matter* **2009,** *30* (1), 83-92.

25. Roorda, W. E.; Bouwstra, J. A.; Devries, M. A.; Junginger, H. E., THERMAL-BEHAVIOR OF POLY HYDROXY ETHYL METHACRYLATE (PHEMA) HYDROGELS. *Pharm. Res.* **1988,** *5* (11), 722-725.

26. Vargun, E.; Sankir, M.; Aran, B.; Sankir, N. D.; Usanmaz, A., Synthesis and Characterization of 2-Hydroxyethyl Methacrylate (HEMA) and Methyl Methacrylate (MMA) Copolymer Used as Biomaterial. *J. Macromol. Sci. Part A-Pure Appl. Chem.* **2010,** *47* (3), 235-240.

27. Miyashita, Y.; Kobayashi, R.; Kimura, N.; Suzuki, H.; Nishio, Y., Transition behavior and phase structure of chitin/poly(2-hydroxyethyl methacrylate) composites synthesized by a solution coagulation bulk polymerization method. *Carbohydr. Polym.* **1997,** *34* (4), 221-228.

28. Rosen, S. L., *Fundamental principles of polymeric materials*. 2nd ed.; Wiley: New York, 1993; p xvi, 420 pages.

29. Hanemann, T.; Szabó, D. V., Polymer-nanoparticle composites: From synthesis to modern applications. *Materials (Basel)* **2010,** *3* (6), 3468-3517.

30. Fox, T. G.; Loshaek, S., Influence of Molecular Weight and Degree of Crosslinking on the Specific Volume and Glass Temperature of Polymers. *J Polym Sci* **1955,** *15* (80), 371-390.

31. Piskun, Y. A.; Vasilenko, I. V.; Zaitsev, K. V.; Oprunenko, Y. F.; Kostjuk, S. V., Synthesis of Functional Poly(epsilon-caprolactone)s via Living Ring-Opening Polymerization of epsilon-Caprolactone Using Functionalized Aluminum Alkoxides as Initiators. *Macromol Chem Phys* **2017,** *218* (7).

32. McGuinness, E. K.; Leng, C. Z.; Losego, M. D., Increased Chemical Stability of Vapor-Phase Infiltrated AlOx-Poly(methyl methacrylate) Hybrid Materials. *Acs Applied Polymer Materials* **2020,** *2* (3), 1335-1344.

33. Gregorczyk, K. E.; Pickup, D. F.; Sanz, M. G.; Irakulis, I. A.; Rogero, C.; Knez, M., Tuning the tensile strength of cellulose through vapor-phase metalation. *Chem. Mater.* **2015,** *27* (1), 181-188.

34. Hill, G. T.; Lee, D. T.; Williams, P. S.; Needham, C. D.; Dandley, E. C.; Oldham, C. J.; Parsons, G. N., Insight on the Sequential Vapor Infiltration Mechanisms of Trimethylaluminum with Poly(methyl methacrylate), Poly(vinylpyrrolidone), and Poly(acrylic acid). *J. Phys. Chem. C Nanomater. Interfaces* **2019,** *123* (26), 16146-16152.

35. Yang, F.; Brede, J.; Ablat, H.; Abadia, M.; Zhang, L.; Rogero, C.; Elliott, S. D.; Knez, M., Reversible and irreversible reactions of trimethylaluminum with common organic functional groups as a model for molecular layer deposition and vapor phase infiltration. *Adv. Mater. Interfaces* **2017,** *4* (18), 1700237.

36. Leng, C. Z.; Losego, M. D., A physiochemical processing kinetics model for the vapor phase infiltration of polymers: measuring the energetics of precursor-polymer sorption, diffusion, and reaction. *Phys. Chem. Chem. Phys.* **2018,** *20* (33), 21506-21514.